Accepted Manuscript

Synthesis of PI3K inhibitor GDC-0077 via a stereocontrolled *N*-arylation of α-amino acids

Chong Han, Sean M. Kelly, Theresa Cravillion, Scott Savage, Tina Nguyen, Francis Gosselin

PII: S0040-4020(19)30476-4

DOI: https://doi.org/10.1016/j.tet.2019.04.057

Reference: TET 30302

To appear in: *Tetrahedron*

Received Date: 10 March 2019

Revised Date: 19 April 2019

Accepted Date: 23 April 2019

Please cite this article as: Han C, Kelly SM, Cravillion T, Savage S, Nguyen T, Gosselin F, Synthesis of PI3K inhibitor GDC-0077 via a stereocontrolled *N*-arylation of α-amino acids, *Tetrahedron* (2019), doi: https://doi.org/10.1016/j.tet.2019.04.057.

Graphical Abstract

Synthesis of PI3K inhibitor GDC-0077 via a stereocontrolled *N*-arylation of α-amino acids

Leave this area blank for abstract info.

Chong Han,* Sean M. Kelly, Theresa Cravillion, Scott J. Savage, Tina Nguyen, and Francis Gosselin
Department of Small Molecule Process Chemistry, Genentech, Inc., 1 DNA Way, South San Francisco, California 94080, United States

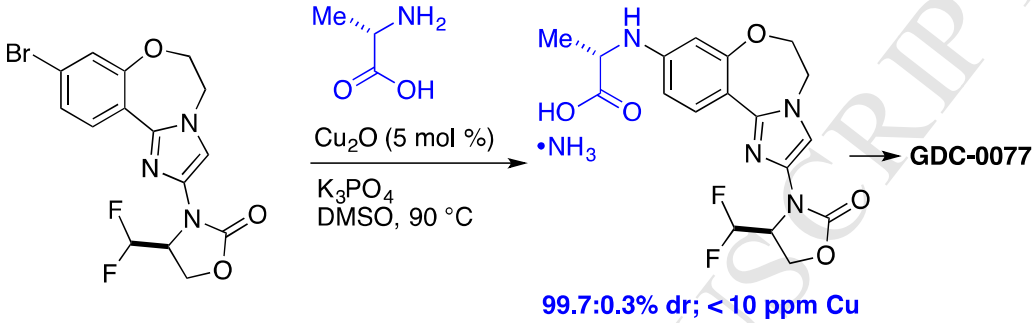

99.7:0.3% dr; < 10 ppm Cu

- *High stereochemical integrity*

Tetrahedron
journal homepage: www.elsevier.com

Synthesis of PI3K inhibitor GDC-0077 via a stereocontrolled *N*-arylation of α-amino acids

Chong Han,* Sean M. Kelly, Theresa Cravillion, Scott Savage, Tina Nguyen, and Francis Gosselin

Department of Small Molecule Process Chemistry, Genentech, Inc., 1 DNA Way, South San Francisco, California 94080, United States

ARTICLE INFO

Article history:
Received
Received in revised form
Accepted
Available online

Keywords:
C−N coupling
N-arylation
Amino acids
Amidation
Stereocontrolled

ABSTRACT

An efficient synthesis of PI3K inhibitor GDC-0077, featuring two consecutive Cu-catalyzed C−N coupling reactions, is reported. The described synthetic route involves a chemoselective Ullmann-type coupling of a chiral difluoromethyl-substituted oxazolidinone, a Cu-catalyzed *N*-arylation of L-alanine with high stereochemical integrity, and a high-yielding final amide bond formation step to produce GDC-0077 in >99.5 area % HPLC purity.

1. Introduction

The phosphoinositide 3-kinase (PI3K) intracellular signaling pathway and its downstream Akt and mTOR cascades have been shown to be activated by mutation in many forms of cancer.[1] Therefore, extensive research efforts have been focusing on designing selective PI3K inhibitors as antitumor agents.[2] GDC-0077 is a potent small molecule PI3Ka inhibitor with excellent PI3K isoform selectivity that is currently in clinical development for the treatment of HR+, HER2- breast cancer (Figure 1). In the medicinal chemistry synthesis, the construction of the imidazole ring and the chemoselective Ullmann-type coupling of difluomethyl-substituted oxazolidinone suffered from moderate yields and selectivity.[3] Moreover, the Cu-catalyzed *N*-arylation of L-alanine was found to be exceedingly oxygen-sensitive and inconsistent, giving variable amounts (up to 30%) of an undesired diastereomer across different batches. In order to produce the GDC-0077 active pharmaceutical ingredient (API) to supply the clinical trials and drug product development needs, we were tasked to develop a robust synthesis amenable to multi-kilogram scale manufacturing.

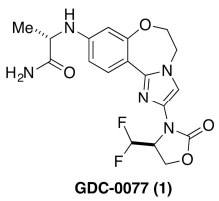

Figure 1. Structure of GDC-0077

2. Results and discussion

Our retrosynthetic analysis of GDC-0077 (**1**) is depicted in Scheme 1. Through the Cu-catalyzed *N*-arylation of L-alanine **2** and a subsequent amide formation using ammonia, the final target would be accessed from aryl bromide **3** which could be prepared from the chemoselective Ullmann-type coupling of the 9-bromo-2-iodo-5,6-dihydrobenzo[*f*]imidazo[1,2-*d*][1,4]oxazepine **4** and oxazolidinone **5**.[4] **4** could then be prepared from the corresponding parent imidazole **6** through an iodination sequence.[5] Leveraging on our reported synthesis of taselisib containing a similar tricyclic 5,6-dihydroimidazobenzoxazepine moiety,[6] imidazole **6** would be derived from a condensation of previously reported cyclic amidine **7** with chloroacetaldehyde **8**.[7]

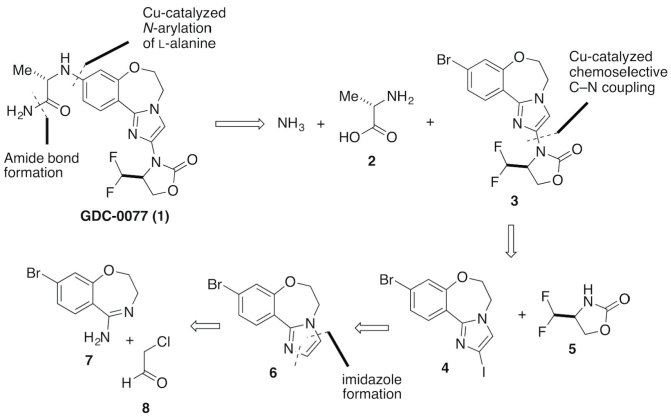

Scheme 1. Retrosynthetic Analysis

The synthesis of **4** is depicted in Scheme 2. Condensation of cyclic amidine **7** with chloroacetaldehyde **8** produced imidazole **6**. Selective iodination using NIS in DMF occurred cleanly at the undesired C-1 position at 25 ºC leading to the formation of positional isomer **10a**. Complete bis-iodination took place at elevated temperature (60 ºC) affording **10b** in 85% yield from **6**, which underwent iodo−magnesium exchange using EtMgBr and subsequent protonation to provide the desired positional isomer **4** cleanly in 82% yield.

Scheme 2. Synthesis of benzoxazepine **4**

Table 1
Optimization of chemoselective Cu-catalyzed coupling reaction of **4** and **5**[a]

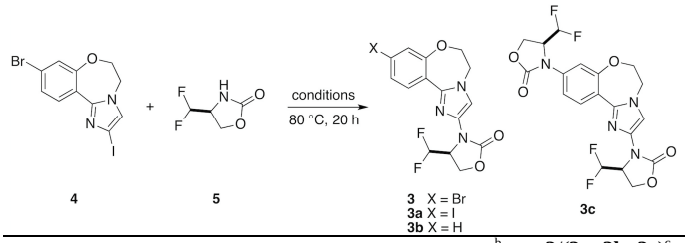

entry	ligand	base	solvent	conv[b] (%)	**3**/(**3a**+**3b**+**3c**)[c] (%)
1	**L1**	K_3PO_4	MeCN	95	74:26
2	**L1**	Cs_2CO_3	MeCN	99	88:12
3	**L2**	Cs_2CO_3	MeCN	99	32:68
4	**L3**	Cs_2CO_3	MeCN	29	99:1
5	**L4**	Cs_2CO_3	MeCN	28	99:1
6	**L5**	Cs_2CO_3	MeCN	4	N/A
7	**L2**	Cs_2CO_3	2-MeTHF	87	98:2
8	**L2**	K_3PO_4	2-MeTHF	99	15:85
9	**L1**	Cs_2CO_3	2-MeTHF	56	97:3
10	**L3**	Cs_2CO_3	2-MeTHF	50	99:1
11[d]	**L2**	Cs_2CO_3	2-MeTHF	98[e]	96:4

[a]Reaction conditions: **4** (1.5 mmol), **5** (1.05 equiv), $Cu(OAc)_2$ (20 mol %), ligand (30 mol %), base (2.0 equiv), solvent (0.5 M).

[b]Determined by HPLC analysis of crude reaction mixture.

[c]Normalized ratio with the total of **3**, **3a**, **3b, and 3c** being 100.

[d]1.1 equiv of **5** used.

[e] 92% assay yield by quantitative HPLC analysis.

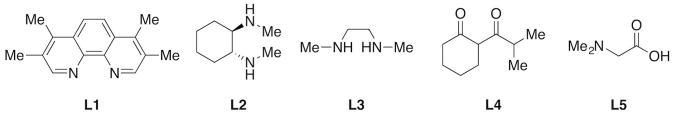

With benzoxazepine **4** in hand, we next evaluated the chemoselective coupling with oxazolidinone **5**. Employing the optimal conditions (K_3PO_4, **L1**, MeCN) described in our published method paper[4] gave 95% conversion but a mixture of desired bromo product **3**, halogen-scrambled iodo product **3a**, des-bromo product **3b**, and bis-coupled product **3c** (Table 1, entry 1). The side products were minimized from a total of 26% to 12% using Cs_2CO_3 instead of K_3PO_4 as the base (entry 2). However, complete removal of the ligand **L1** proved to be challenging through downstream aqueous work-ups or crystallization, requiring purification by column chromatography. Evaluation of other aqueous soluble ligands **L2**–**L5** proved fruitless due to excessive halogen scrambling or low conversion (entries 3−6). We next turned to a high-throughput experimentation (HTE) approach in search of alternative reaction conditions. A survey of a full combination of 8 ligands, 3 bases, and 8 solvents in two 96-well plates revealed interesting conditions consisting of **L2** as the ligand, Cs_2CO_3 as the base, and 2-MeTHF as the solvent. In contrast to previously disclosed results showing a high bromo−iodo scrambling rate using **L2**[4,8] as the ligand in either DMSO or MeCN, the reaction was found to be very clean when 2-MeTHF was employed as the solvent and Cs_2CO_3 was used as the base (entry 7−10) regardless of the ligands used. The fastest reaction rate could be obtained using **L2** as the ligand (87% conversion by HPLC analysis) and further increasing the stoichiometry of oxazolidinone **5** to 110 mol % gave 98% conversion and 92% assay yield of the desired product **3** ascertained by quantitative HPLC analysis (entry 11).

Table 2
Optimization of Cu-catalyzed coupling reaction of **2** and **3**[a]

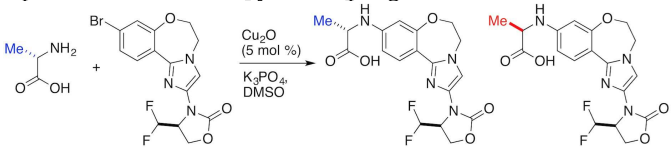

entry	**2** (equiv)	ancillary ligand	temp (°C)	time (h)	conv.[b]	dr[b]
1	2.0	-	100	2	92	94:6
2	3.0	-	100	2	99[c]	98:2
3	3.0	**L2**	90	1	83	95:5
4	3.0	**L4**	90	1	88	94:6
5	3.0	**L5**	90	1	83	95:5
6	3.0	-	90	2	92	95:5
7	3.0	-	80	5	91	87:13

[a]Reaction conditions: **3** (1 mmol), **2** (1.2 equiv), Cu_2O (5 mol %), ancillary ligand (20 mol %), K_3PO_4 (3.0 equiv), solvent (0.5 M).

[b]Determined by HPLC analysis of crude reaction mixture.

[c]90% assay yield by quantitative HPLC analysis.

We next focused on the coupling of L-alanine (**2**) with aryl bromide **3** (Table 2). Pioneering work by Ma and co-workers highlighted a dual role of α-amino acids as both the reactants and the accelerating ligands in the Cu-catalyzed *N*-arylation reaction.[9] A number of examples were subsequently reported from various groups,[10] including several in which additional ancillary ligands were utilized.[11] However, only a few studied the stereochemical integrity of the *N*-aryl amino acid products.[12]

Initial experiments revealed poor reproducibility with respect to the level of stereochemical erosion (3−30%) leading to the undesired diastereomer **11a′**, which was attributed to the extreme oxygen sensitivity for this coupling reaction. Evaluation of a variety of copper salts including CuI, CuBr, Cu_2O, $Cu(OAc)_2$, CuO, $CuSO_4$ led us to focus on Cu_2O for further optimization as it showed the best oxygen tolerability. Under a strictly inert atmosphere, use of 3.0 equiv of L-alanine (**2**) further mitigated the risk of stereochemical erosion, providing a 98:2 dr of product **11a** as opposed to a 94:6 dr when 2 equiv were used. (Table 2, entry 2 vs entry 1). Additional ancillary ligands **L2**, **L4**, and **L5** were examined but showed no improvement with respect to

either reaction rate or dr (entries 3–6). We also observed lower dr when the reaction was performed at temperatures below 100 ºC (entries 6–7 vs 2).

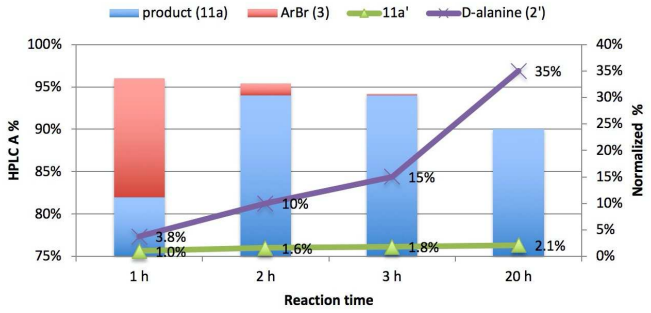

Figure 2. A time course experiment to probe the cause of stereochemical erosion

Preliminary mechanistic investigation via an experiment monitoring the level of **11a′** and D-alanine (**2′**) throughout the course of the reaction revealed the origin of stereochemical erosion was presumably due to racemization of L-alanine rather than epimerization of product **11a**. As shown in Figure 2 with conversion of ArBr (**3**) to product (**11a**) shown in stacked columns on the primary y-axis to the left and normalized percentage of eroded stereoisomers (**11a′ or 2′**) in marked lines reflecting dr or er on the second y-axis to the right, the level of undesired diastereomer **11a′** remained at approximately the same level once the starting material **3** was completely consumed after 2–3 h, while the unreacted L-alanine (**2**) in excess continued racemizing to the corresponding D-alanine (**2′**), reaching to a 35:65 er after 20 h. The experimental results were in accord with the proposed reaction pathway (Scheme 3) in which the D-alanine (**2′**) derived from racemization of **2** reacted with aryl bromide **3** leading to the formation of the undesired diastereomer **11a′**.

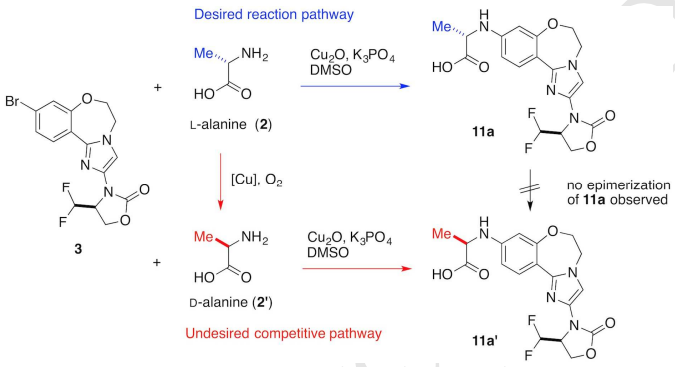

Scheme 3. Proposed reaction pathway for the formation of undesired diastereomer **11a′**

Under the optimized conditions, the level of undesired diastereomer **11a′** could be controlled at an average of approximately 3% over multiple development runs on a decagram scale (Figure 3). Further investigation on the temperature dependence of the stereochemical erosion revealed L-alanine (**2**) racemized at an appreciable rate above 60 ºC while the desired *N*-arylation of **3** was quite slow below 70 ºC. This intrinsic reactivity difference posed an additional challenge to minimize stereochemical erosion when scaling up the process in a batch mode, because it would take a longer time to heat the batch to the desired reaction temperature on a kilogram scale compared to the laboratory runs. We envisioned two potential solutions to circumvent this issue: charging L-alanine (**2**) or Cu_2O catalyst last to a reaction mixture preheated to 90–100 ºC. The latter approach was deemed more practical to implement in a pilot plant and showed further improved robustness with an average of approximately 1% of **11a′** over multiple development runs on a decagram scale (Figure 3).

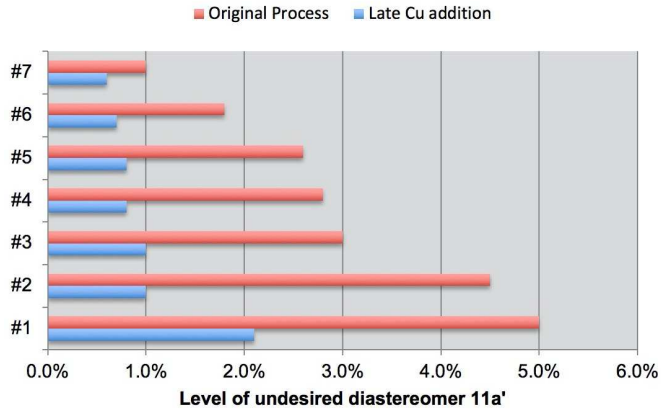

Figure 3. Reproducibility of Cu-catalyzed coupling of **2** and **3**. Level of the undesired diastereomer **11a′** determined by HPLC analysis of crude reaction mixtures.

Even with the extensive optimization of the reaction conditions for the Cu-catalyzed coupling of **2** and **3**, further purging of the undesired diastereomer **11a′** would still be required before conversion to the final product **GDC-0077** (**1**) for two reasons: no observed depletion of the resulting diastereomer in the final stage and the exceedingly high purity requirement for the API. Moreover, although the corresponding potassium salt of **11a** was found to be very stable, attempt to isolate **11a** in its free acid form via crystallization unveiled its extreme oxygen sensitivity with the major degradation product identified as the aniline **12b**, presumably through an oxidative decarboxylation pathway analogous to Strecker degradation[13] via intermediate **12a** (Scheme 4).[14] We resorted to an HTE approach in search for a salt of **11a** to improve its stability and further lower the level of **11a′**. The corresponding ammonium salt **11b** was identified to demonstrate excellent purging power of **11a′** from a wide range of starting levels: reducing **11a′** to 4% from as high as 21% and reducing to 0.5% from a 2% starting level (Figure 4).

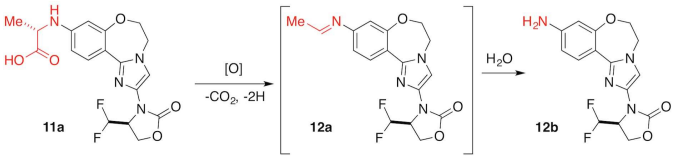

Scheme 4. Proposed degradation pathway from **11a** to **12b**

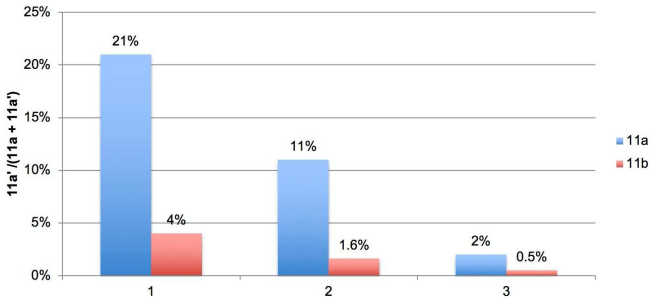

Figure 4. Purging of undesired diastereomer **11a′** via isolation of ammonium salt **11b**

We suspected another contributing factor to the instability of **11a** was the residual copper serving as a catalyst for the oxidative degradation pathway. A survey of aqueous washes including ammonium hydroxide or ammonium chloride during workup to

scavenge the copper led to a high loss of product in the aqueous layer. Evaluation of solid-based metal scavengers in THF identified SiliaMet® DMT[15] as the best hit. At 40 wt % scavenger loading relative to the mass of **11a**, the residual copper level could be reduced from >3000 ppm to <10 ppm. The effective copper purging, in conjunction with the formation of the corresponding ammonium salt **11b**, significantly improved the overall stability of free acid **11a**. As shown in Figure 5, no noticeable degradation was observed when a sample of **11b** with 8 ppm residual Cu was stored on benchtop over 7 days. It is noteworthy that even copper-free **11a** (< 3ppm) was found to be unstable in our hands.

Figure 5. Stability comparison of free acid **11a** and corresponding ammonium salt **11b**

Table 3 Optimization of amide formation to produce **1**[a]

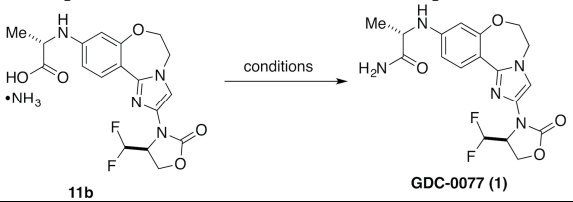

entry	SM	coupling reagent (equiv)	NH_3 source	temp	conv[b] (%)	yield[c] (%)
1	**11a**	CDI	NH_4OH	0	100	97
2	**11b**	CDI	NH_4OH	0	70	40
3	**11b**	T3P®	NH_3/MeOH	0	43	23
4	**11b**	HATU	NH_3/MeOH	0	99	63
5	**11b**	EDC/HOBt	NH_3/MeOH	0 to 25	97	89
6	**11b**	EDC/HOPy	NH_3/MeOH	0 to 25	27	1
7	**11b**	EDC/NMI	NH_3/MeOH	0 to 25	20	2
8	**11b**	EDC/DMAP	NH_3/MeOH	0 to 25	11	2
9	**11b**	EDC/HOSu	NH_3/MeOH	0 to 25	98	92
10	**11b**	EDC/HOSu	NH_3/*i*-PrOH	10	99	96

[a]Reaction conditions: **11a or 11b** (1 mmol), coupling reagent (2.0 equiv), nucleophilic activator (1.0 equiv, used in the cases where EDC was the coupling reagent), NH_3 source (1.0 equiv), THF (0.24 M).

[b]Determined by HPLC analysis of crude reaction mixture.

[c]Quantitative assay yield based on HPLC analysis.

With a robust process developed to prepare **11b** in high purity, we began evaluating reaction conditions for the final amidation step (Table 3). Although initial experiment using CDI as the coupling reagent yielded a clean reaction for acid **11a** (entry 1), the reaction starting with the ammonium salt **11b** gave only 70% conversion and 40% yield under identical conditions (entry 2) due to the incompatibility between CDI and the ammonium ion. Since it was highly desirable to use the isolated ammonium salt **11b** as the starting material to avoid an extra salt breaking step to reform the corresponding acid **11a** in situ, we next focused on evaluating milder amidation conditions compatible with **11b** including T3P®, HATU, EDC in conjunction with nucleophilic activators (entries 3−9). As a result, the reactions using EDC as the dehydrating reagent and HOBt (entry 5) or HOSu (entry 9) as the nucleophilic activator provided the best conversion and yield using NH_3 in MeOH. Switching out the ammonia source to NH_3 in more sterically hindered *i*-PrOH eliminated the formation of the corresponding methyl ester of **11a** improving the assay yield from 92% to 96% (entries 9 and 10).

With all the previous optimization efforts, we were able to develop a robust process amenable to kilogram-scale manufacturing illustrated in Scheme 5. Chemoselective C−N coupling between **4** and **5** under optimized conditions led to compound **3** in 77% yield with minimized Br−I scrambling. Subsequent coupling of **3** with L-alanine (**2**) under the optimized conditions followed by copper scavenging and salt formation afforded the ammonium salt **11b** in 81% yield with high stereochemical integrity and much improved stability. Examination of reaction conditions for the final amidation step identified the best EDC/HOSu combination using NH_3 in *i*-PrOH to provide **GDC-0077** API in 83% yield and >99.5% purity ascertained by HPLC analysis.

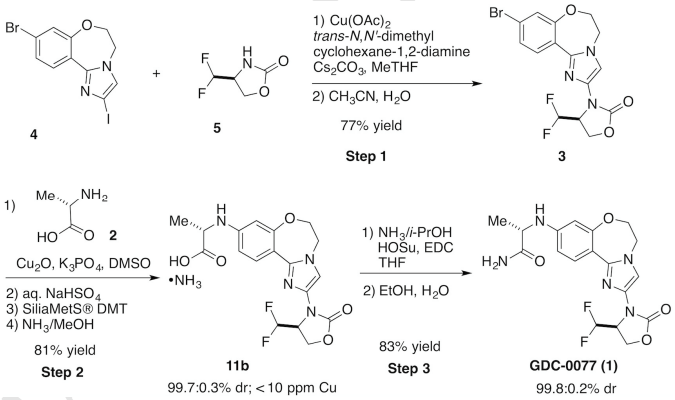

Scheme 5. Synthesis of GDC-0077

3. Conclusion

In summary, we developed an efficient and robust process to synthesize the **GDC-0077** API featuring two consecutive Cu-catalyzed C−N couplings in chemoselective and stereocontrolled manner. The scalability and robustness of the developed process was successfully demonstrated on multi-kilogram scale. Further mechanistic studies are underway to understand the mechanism of Cu-catalyzed L-alanine racemization.

4. Experimental section

4.1. General

Unless stated otherwise, reactions were performed under an ambient atmosphere of nitrogen in 20 mL vials sealed with Teflon-lined caps. All solvents and commercially obtained reagents were used as received, unless specified otherwise. Thin-layer chromatography (TLC) was conducted with EMD silica gel 60 F254 pre-coated plates and visualized using UV light (254 nm). Flash column chromatography was performed with pre-packed RediSep silica gel columns on a CombiFlash ISCO system using MeOH in CH_2Cl_2 (0−5% gradient) as eluent. Analytical HPLC analyses were performed with an Agilent 1290 Infinity Series HPLC instrument. ^{1}H NMR spectra were recorded on a Bruker 500 (at 500 MHz) and are reported relative to the residual solvent peak (δ 2.50 for DMSO-d_6). Data for ^{1}H NMR spectra are reported as follows: chemical shift (δ ppm), multiplicity, coupling constant (Hz), and integration. ^{13}C NMR spectra were recorded on a Bruker 500 (at 126 MHz), and are reported relative the residual solvent peak (δ 39.5 for DMSO-d_6). Data for ^{13}C NMR spectra are reported in terms of chemical shift (δ ppm), multiplicity, and coupling constant (Hz) due to fluorine

splitting. IR spectra were recorded on a Bruker Alpha Platinum-ATR spectrometer and are reported in frequency of absorption (cm^{-1}). HRMS data was obtained on an LTQ Orbitrap Discovery (Thermo Fisher Scientific) at Genentech, Inc. Melting points were measured by differential scanning calorimetry (DSC) and were reported as onset temperature.

4.2. Procedure for preparation of GDC-0077 (1)

*9-bromo-5,6-dihydrobenzo[f]imidazo[1,2-d][1,4]oxazepine (**6**):* Into a mixture of 8-bromo-2,3-dihydrobenzo[*f*][1,4]oxazepin-5-amine hydrochloride (17.6 kg, 63.4 mol, 100 mol %) and 2-MeTHF (122 kg) were charged a 40% chloroacetaldehyde aqueous solution (16.4 kg, 132 mol %) and water (10 kg). The mixture was heated to 40 ºC and aqueous $KHCO_3$ solution was charged. The reaction mixture was stirred at 45 ºC for 21 h. After the reaction was complete, the reaction mixture was cooled to 20 °C, stirred for 30 min, and filtered. The resulting cake was rinsed with 2-MeTHF (33.0 kg) and the combined filtrates were allowed to settle. The resulting organic layer was washed with aqueous $NaHSO_3$ solution (30 kg), concentrated to approximately 26 L under reduced pressure below 45 ºC. After the addition of DMF (25 kg), the mixture was concentrated to approximately 26 L under reduced pressure below 45 ºC. Water (154 kg) was charged at 40 ºC followed by seeding with 9-bromo-5,6-dihydrobenzo[*f*]imidazo[1,2-*d*][1,4]oxazepine (1.20 kg). The mixture was stirred at 40 ºC for another 1.5 h and cooled to 20 ºC. After stirring for 10 h at 20 ºC, the suspension was filtered. The resulting solid was washed with water twice (25 kg × 2) and dried under reduced pressure at 45 ºC to afford 9-bromo-5,6-dihydrobenzo[*f*]imidazo[1,2-*d*][1,4]oxazepine (16.3 kg, 97.5 wt %, 95% yield). mp 121 °C; ^{1}H NMR (500 MHz, DMSO-d_6) δ 8.33 (d, *J* = 8.6 Hz, 1H), 7.34 (d, *J* = 1.1 Hz, 1H), 7.28 (dd, *J* = 8.6, 2.1 Hz, 1H), 7.24 (d, *J* = 2.1 Hz, 1H), 7.06 (d, *J* = 1.1 Hz, 1H), 4.50 – 4.39 (m, 4H); ^{13}C NMR (126 MHz, DMSO-d_6) δ 156.0, 142.9, 131.5, 129.1, 125.7, 123.6, 123.4, 121.7, 118.7, 69.4, 49.6; HRMS calcd for $C_{11}H_{10}BrN_2O$ $[M+H]^+$: 264.9971, found 264.9976.

*9-bromo-2,3-diiodo-5,6-dihydrobenzo[f]imidazo[1,2-d][1,4]oxazepine (**10b**):* Into a solution of 9-bromo-5,6-dihydrobenzo[*f*]imidazo[1,2-*d*][1,4]oxazepine (16.3 kg, 97.5 wt %, 59.9 mol, 100 mol %) in DMF (78.0 kg) was added NIS (29.0 kg, 215 mol %) at 40 ºC. The reaction mixture was slowly heated to 70 ºC and stirred for 6 h. After the reaction was complete, 10% aqueous Na_2SO_3 solution (78.0 kg) was charged at 45 ºC followed by water (154 kg). The resulting suspension was stirred at 45 ºC for 1 h and cooled to 20 ºC. After stirring at 20 ºC for 8 h, the suspension was filtered. The resulting solid was washed with water (160 kg) and dried under reduced pressure at 45 ºC to afford 9-bromo-2,3-diiodo-5,6-dihydrobenzo[*f*]imidazo[1,2-*d*][1,4]oxazepine (29.7 kg, 100 wt %, 96% yield) as an off-white solid. mp 180 °C; ^{1}H NMR (500 MHz, DMSO-d_6) δ 8.21 (d, *J* = 8.7 Hz, 1H), 7.32–7.24 (m, 2H), 4.53–4.44 (m, 2H), 4.40–4.31 (m, 2H); ^{13}C NMR (126 MHz, DMSO-d_6) δ 156.5, 147.1, 131.2, 125.9, 123.4, 122.8, 117.2, 98.4, 89.7, 69.2, 53.5; HRMS calcd for $C_{11}H_8BrI_2N_2O$ $[M+H]^+$: 516.7904, found 516.7911.

*9-bromo-2-iodo-5,6-dihydrobenzo[f]imidazo[1,2-d][1,4]oxazepine (**4**):* Into a solution of 9-bromo-2,3-diiodo-5,6-dihydrobenzo[*f*]imidazo[1,2-*d*][1,4]oxazepine (39.4 kg, 76.2 mol, 100 mol %) in THF (180 kg) was added a solution of 2.0 M EtMgBr in 2-MeTHF (44.0 kg, 120 mol %) at 10 ºC. The reaction mixture was stirred at 10 ºC for 2 h. After the reaction was complete, 5% aqueous HOAc (133 kg) was charged while maintaining the batch temperature below 30 ºC. EtOAc (168 kg) was charged and the resulting mixture was stirred at 20 ºC for 1 h. The layers were separated and the aqueous layer was extracted with EtOAc (77.8 kg). The combined organic layers were washed with water (76.0 kg) and filtered through a pad of silica gel (19.8 kg). The silica gel pad was rinsed with EtOAc (69.6 kg). The combined filtrates were concentrated to approximately 100 L under reduced pressure below 50 ºC and THF (146 kg) was added. The resulting mixture was heated to 60 ºC until a clear solution was obtained before it was concentrated to approximately 100 L under reduced pressure below 50 ºC and then cooled to 30 ºC. *n*-Heptane was charged (86.8 kg) and the resulting mixture was stirred at 30 ºC for 2 h. The batch was solvent-switched to *n*-heptane by three cycles of batch concentration under reduced pressure below 35 ºC to approximately 180 L and *n*-heptane addition (47.6 kg × 3). The resulting suspension was cooled to 20 ºC, stirred for 12 h, and filtered. The resulting solid was washed with *n*-heptane (64.0 kg) and dried under reduced pressure at 45 ºC to afford 9-bromo-2-iodo-5,6-dihydrobenzo[*f*]imidazo[1,2-*d*][1,4]oxazepine (25.3 kg, 98.7 wt %, 84% yield) as a light tan solid. mp 165 °C; ^{1}H NMR (500 MHz, DMSO-d_6) δ 8.22 (d, *J* = 8.7 Hz, 1H), 7.55 (s, 1H), 7.31–7.23 (m, 2H), 4.48–4.39 (m, 4H); ^{13}C NMR (126 MHz, DMSO-d_6) δ 156.0, 145.1, 131.4, 128.9, 125.8, 123.5, 122.4, 117.4, 83.7, 69.1, 49.8; HRMS calcd for $C_{11}H_9BrIN_2O$ $[M+H]^+$: 390.8937, found 390.8949.

*(S)-3-(9-bromo-5,6-dihydrobenzo[f]imidazo[1,2-d][1,4]oxazepin-2-yl)-4-(difluoromethyl)oxazolidin-2-one (**3**):* 9-bromo-2-iodo-5,6-dihydrobenzo[*f*]imidazo[1,2-*d*][1,4]oxazepine (6.90 kg, 98.7 wt %, 17.4 mol, 100 mol %) was charged to a reactor, followed by (*S*)-4-(difluoromethyl)oxazolidin-2-one (2.68 kg, 112 mol %), $Cu(OAc)_2$ (0.653 kg, 20.6 mol %), and Cs_2CO_3 (11.7 kg, 206 mol %). The reactor was evacuated and backfilled with N_2 three times. 2-MeTHF (36.0 kg) and *trans-N,N*-dimethylcyclohexane-1,2-diamine (0.764 kg, 30 mol %) was then charged into the reactor. The reactor was evacuated and backfilled with N_2 three times. The reaction mixture was heated to 78 ºC and stirred for 22 h. After the reaction was complete, a 20 wt % $NaHSO_4$ aqueous solution (42.0 kg) was slowly added while maintaining the internal temperature between 60–70 ºC. The layers were separated at 65 ºC and the aqueous layer was removed. The batch was solvent-switched to MeCN via a constant volume distillation under reduced pressure at 60–70 ºC by adding MeCN (62.3 kg). Water (14.1 kg) was added into the reactor while maintaining the batch temperature between 60–70 ºC. The suspension was cooled to 20 °C at a rate of 0.5 ºC/min, stirred for 18 h, and filtered. The resulting solid was washed with a mixture of MeCN and water (50 kg, 44:56, w/w) and dried under reduced pressure at 90 ºC to afford (*S*)-3-(9-bromo-5,6-dihydrobenzo[*f*]imidazo[1,2-*d*][1,4]oxazepin-2-yl)-4-(difluoromethyl)oxazolidin-2-one as a tan solid (5.85 kg, 91.9 wt %, 77% yield); mp 247 °C; ^{1}H NMR (500 MHz, DMSO-d_6) δ 8.26 (d, *J* = 8.7 Hz, 1H), 7.40 (s, 1H), 7.33–7.23 (m, 2H), 6.85–6.60 (m, 1H), 5.00 (ddd, *J* = 22.9, 8.7, 4.2 Hz, 1H), 4.66 – 4.55 (m, 2H), 4.47 (q, *J* = 5.9, 4.3 Hz, 4H).; ^{13}C NMR (126 MHz, DMSO-d_6) δ 156.3, 154.4, 139.3, 136.3, 131.6, 125.8, 123.4, 122.1, 117.8, 116.1–111.4 (m), 109.9, 69.2, 62.0, 55.8 (dd, *J* = 31.0, 21.5 Hz), 50.1; HRMS calcd for $C_{15}H_{13}BrF_2N_3O_3$ $[M+H]^+$: 400.0103, found 400.0134.

*ammonium (S)-2-((2-((S)-4-(difluoromethyl)-2-oxooxazolidin-3-yl)-5,6-dihydrobenzo[f]imidazo[1,2-d][1,4]oxazepin-9-yl) amino)propionate (**11b**):* (*S*)-3-(9-bromo-5,6-dihydrobenzo[*f*]imidazo[1,2-*d*][1,4]oxazepin-2-yl)-4-(difluoromethyl) oxazolidin-2-one **3** (3.96 kg, 91.9 wt %, 9.19 mol, 100 mol %) was charged to a reactor, followed by (*S*)-2-aminopropanoic acid (2.49 kg, 307 mol %), anhydrous K_3PO_4 (5.84 kg, 303 mol %), and DMSO (19.9 kg). The mixture was sparged with N_2 for 1 h and heated to 95 ºC. A slurry of Cu_2O

(67.1 g, 5.16 mol %) in DMSO (2.21 kg) that was pre-sparged with N_2 for 30 min was then transferred to the reactor. The reaction mixture was stirred at 95 ºC for 4 h. After the reaction was complete, the reaction mixture was cooled to 20 ºC. DCM (37.3 kg) was added to the reactor, followed by water (24.2 kg). The layers were separated and the organic layer was removed. The aqueous layer was washed with DCM (26.6 kg) one more time. THF (35.2 kg) and an aqueous $NaHSO_4$ solution (19 wt %, 20.7 kg) were charged to the reactor sequentially. The layers were separated and the aqueous layer was removed. The organic layer was washed with 15 wt % brine (2 × 12 kg). SiliaMetS® DMT (Silicycle Inc., 1.60 kg) was charged and the batch was stirred at 25 ºC for 15 h and filtered to scavenge residual metal. THF (24.8 kg) was used to rinse the filter. The combined filtrates were heated to 50 ºC. A 7 N solution of NH_3 in MeOH (1.02 kg, 100 mol %) was added followed by a slurry of seeds (**11b**, 19.5 g) in THF (0.395 kg). The resulting suspension was stirred at 50 ºC for 2 h and a constant volume distillation was conducted at 40–60 ºC under reduced pressure to remove residual water by adding anhydrous THF (60.1 kg). A 7 N solution of NH_3 in MeOH (1.02 kg, 100 mol %) was added. The suspension was stirred at 50 ºC for 15 h and filtered. The resulting solid was washed with THF (21.8 kg) and dried under reduced pressure at 25 ºC to afford ammonium (*S*)-2-((2-((*S*)-4-(difluoromethyl)-2-oxooxazolidin-3-yl)-5,6-dihydrobenzo[*f*]imidazo[1,2-*d*][1,4]oxazepin-9-yl)amino)propionate **11b** as a beige solid (3.19 kg, 98.0 wt %, 81% yield, 99.7:0.3 dr). mp = 171 °C; ^{1}H NMR (500 MHz, DMSO-d_6) δ 7.97 (d, *J* = 8.8 Hz, 1H), 7.16 (s, 1H), 6.74–6.69 (m, 1H), 6.38 (dd, *J* = 9.0, 2.2 Hz, 1H), 6.07 (d, *J* = 2.2 Hz, 1H), 5.02–4.91 (m, 1H), 4.64–4.52 (m, 2H), 4.40–4.30 (m, 4H), 3.63 (q, *J* = 6.1, 5.5 Hz, 1H), 1.27 (d, *J* = 6.7 Hz, 3H); ^{13}C NMR (126 MHz, DMSO-d_6) δ 176.3, 157.3, 154.4, 150.2, 141.7, 135.5, 130.8, 113.7 (t, *J* = 244.1 Hz), 109.0, 107.5, 105.8, 101.5, 68.6, 61.8, 55.8 (dd, *J* = 31.6, 21.1 Hz), 53.1 (d, *J* = 2.6 Hz), 50.0, 19.3; HRMS calcd for $C_{18}H_{19}F_2N_4O_5$ $[M+H]^+$: 409.1318, found 409.1318.

HPLC method for dr determination of compound **11a** or **11b**: column, Waters XBridge C18 (150 × 3 mm, 3.5 µm); temperature, 35 °C; flow rate, 1.0 mL/min; injection volume, 5 µL; detection, 215 nm; mobile phase A, 0.1% phosphoric acid in water; mobile phase B, acetonitrile, gradient (20 min), 0–5 min = 2–10% B, 5–10 min = hold 22% B, 10–15 min = 22–95% B, 15–18 min = hold 95% B, 18–20 min = 2% B. tR of **11a** = 8.633 min, tR of **11a′** = 9.108 min.

*(S)-2-((2-((S)-4-(difluoromethyl)-2-oxooxazolidin-3-yl)-5,6-dihydrobenzo[f]imidazo[1,2-d][1,4]oxazepin-9-yl)amino)propanamide (**GDC-0077, 1**):* Ammonium (*S*)-2-((2-((*S*)-4-(difluoromethyl)-2-oxooxazolidin-3-yl)-5,6-dihydrobenzo[*f*]imidazo[1,2-*d*][1,4]oxazepin-9-yl)amino)propionate **17** (5.60 kg, 13.2 mol, 100 mol %) was charged to a reactor, followed by *N*-hydroxysuccinimide (HOSu, 1.52 kg, 102 mol %) and THF (49.6 kg). The batch was sparged with N_2 for 40 min and cooled to 10 ºC. A 2 N solution of NH_3 in *i*-PrOH (5.05 kg, 101 mol %) and *N*-(3-dimethylaminopropyl)-*N′*-ethylcarbodiimide hydrochloride (EDC, 5.20 kg, 210 mol %) were charged sequentially to the reactor. The reaction mixture was stirred at 10 ºC for 20 h. After the reaction was complete, the mixture was warmed up to 20 ºC and 15 wt % brine (33.7 kg) was added. The layers were separated at 35 ºC and the aqueous layer was removed. The organic layer was washed sequentially with 15 wt % brine (2 × 16.9 kg) and a mixture of 15 wt % brine (8.97 kg) and 28.0–30.0 wt % NH_4OH (7.55 kg) and then filtered through a polishing filter unit. The filter unit was rinsed with THF (5.05 kg). The combined filtrates were distilled under reduced pressure at 50 ºC to approximately half of its original volume. EtOH (8.90 kg) was charged at 50 ºC, followed by a slurry of seeds (**1**, 27.1 g) in ethanol (0.340 kg). The resulting suspension was stirred at 50 ºC for 30 min and solvent-switched to EtOH via a constant volume distillation under reduced pressure at 40–60 ºC by adding EtOH (39.9 kg). Water (0.379 kg) was added at 50 ºC. The suspension was cooled to 20 ºC, stirred for 23 h, and filtered. The resulting solid was washed with a 90:10 (w/w) mixture of EtOH and water (27.9 kg) and dried under reduced pressure at 80 ºC to afford (*S*)-2-((2-((*S*)-4-(difluoromethyl)-2-oxooxazolidin-3-yl)-5,6-dihydrobenzo[*f*]imidazo[1,2-*d*][1,4]oxazepin-9-yl)amino)propanamide **1** as a light pink solid (4.37 kg, 99.7 wt %, 83% yield, 99.8:0.2 dr). mp 214 °C; ^{1}H NMR (500 MHz, DMSO-d_6) δ 8.01 (d, *J* = 8.8 Hz, 1H), 7.38 (d, *J* = 2.4 Hz, 1H), 7.18 (s, 1H), 7.01 (d, *J* = 2.3 Hz, 1H), 6.88–6.59 (m, 1H), 6.42 (dd, *J* = 8.8, 2.4 Hz, 1H), 6.16 (d, *J* = 7.1 Hz, 1H), 6.10 (d, *J* = 2.3 Hz, 1H), 5.02–4.90 (m, 1H), 4.64–4.53 (m, 2H), 4.35 (tdd, *J* = 6.8, 3.9, 1.7 Hz, 4H), 3.78 (p, *J* = 6.9 Hz, 1H), 1.32 (d, *J* = 6.8 Hz, 3H); ^{13}C NMR (126 MHz, DMSO-d_6) δ 176.2, 157.2, 154.4, 149.9, 141.5, 135.6, 130.8, 116.8–110.8 (m), 109.3, 107.8, 106.9, 102.0, 68.7, 61.8, 55.9 (dd, *J* = 31.2, 21.2 Hz), 52.6, 50.0, 19.2; HRMS calcd for $C_{18}H_{20}F_2N_5O_4$ $[M+H]^+$: 408.1478, found 408.1473.

HPLC method for dr determination of compound **1** (**GDC-0077**): column, Ascentis Express C18 column (150 × 4.6 mm, 2.7 µm); temperature, 30 °C; flow rate, 1.0 mL/min; injection volume, 5 µL; detection, 215 nm; mobile phase A, 5 mM phosphate buffer pH=7; mobile phase B, methanol, gradient (30 min), 0–10 min = 2–50% B, 10–15 min = hold 50% B, 15–20 min = 50–85% B, 20–25 min = hold 85% B, 25–30 min = 2% B. tR of **1** = 12.2 min, tR of **1′** (diastereomer) = 12.6 min.

Acknowledgments

We thank Dr. Haiming Zhang for proofreading the manuscript, Dr. Mohammad Al-Sayah and Ms. Meenakshi Goel for analytical support, and Dr. Sarah Robinson for collecting HRMS data (Genentech, Inc.).

Supplementary Material

Supplementary data associated with this article including copies of ^{1}H and ^{13}C NMR spectra can be found in the online version, at http://dx.doi.org.

References and notes

1. For a review, see: V.R. Sharma, G.K. Gupta, A.K. Sharma, N. Batra, D.K. Sharma, A. Joshi, A.K. Sharma, Curr. Pharm. Des. 23 (2017) 1633−1638.
2. For reviews, see: a) J.-E. Kurtz, I. Ray-Coquard, Anticancer Res. 32 (2012) 2463−2470; b) R. Dienstmann, J. Rodon, V. Serra, J. Tabernero, Mol. Cancer Ther. 13 (2014) 1021−1031.
3. M.-G. Braun, E. Hanan, S.T. Staben, R.A. Heald, C. MacLeod, R. Elliott, U.S. Patent Application (2017) 20170210733.
4. For chemoselective coupling of oxazolidinones with bromoiodoarenes, see: S.M. Kelly, C. Han, L. Tung; F. Gosselin, Org. Lett. 19 (2017) 3021−3024 and references cited therein.
5. C.O. Ndubaku, T.P. Heffron et. al., J. Med. Chem. 56 (2013) 4597−4610.
6. F. St-Jean, T. Remarchuk, R. Angelaud, D.E. Carrera, D. Beaudry, S. Malhotra, A. McClory, A. Kumar, G. Ohlenbusch, A. Schuster, F. Gosselin. Org. Process Res. Dev. 23 (2019) ASAP, DOI: 10.1021/acs.oprd.9b00050.
7. For $Mg(OEt)_2$ promoted conversion of nitriles to amidines and its application to imidazole synthesis, see: M.E. Dalziel, J.A. Deichert, D.E. Carrera, D. Beaudry, C. Han, H. Zhang, R. Angelaud, Org. Lett. 20 (2018) 2624−2627.
8. A. Klapars, S.L. Buchwald, J. Am. Chem. Soc. 124 (2002) 14844−14845.
9. D. Ma, Y. Zhang, J. Yao, S. Wu, F. Tao, J. Am. Chem. Soc. 120 (1998) 12459−12467.
10. a) N. Narendar, S. Velmathi, Tetrahedron Lett. 50 (2009) 5159−5161; b) H. Wang, Y. Jiang, K. Gao, D. Ma, Tetrahedron 65 (2009) 8956−8960; c) J. Haynes-Smith, I. Diaz, K.L. Billingsley, Org. Lett. 18 (2016) 2008−2011.
11. a) Z. Lu, R.J. Twieg, Tetrahedron Lett. 46 (2005) 2997−3001; b) Q. Jiang, D. Jiang, Y. Jiang, H. Fu, Y. Zhao, Synlett (2007) 1836−1842; c) K.K. Sharma, S. Sharma, A. Kudwal, R. Jain, Org. Biomol. Chem. 13 (2015) 4637−4641.
12. a) H. Xu, C. Wolf, Chem. Comm. (2009) 1715−1717; b) F. Ma, X. Xie, L. Ding, J. Gao, Z. Zhang, Tetrahedron 67 (2011) 9405−9410; c) S.M. King, S.L. Buchwald, Org. Lett. 18 (2016) 4128−4131.
13. A. Schönberg, R. Moubacher, Chem. Rev. 50 (1952) 261−277.
14. C. Thomas, M. Wu, K.L. Billingsley, J. Org. Chem. 81 (2016) 330−335.
15. Silia*MetS*® DMT is the silica-bound equivalent of 2,4,6-trimercaptotriazine (trithiocyanuric acid, TMT), and a versatile metal scavenger for a variety of metals including ruthenium catalysts and hindered Pd complexes.